Bulgarian Chemical Communications, Volume 47, Special Issue D (pp. 93 – 98) 2015

First-principles calculation of stacking fault energies and mechanical properties for high entropy solid solution $Al_xCoCrCuFeNi$ with different mole fraction of Al

Lan-xin Wang[1], Shan Yao[1*], Bin Wen[2]

[1]*School of Materials Science and Engineering, Dalian University of Technology, Dalian 116023, China*
[2]*State Key Laboratory of Metastable Materials Science and Technology, Yanshan University, Qinhuangdao 066004, China*

Received June 26, 2015, Revised September 10, 2015

The ab initio calculations have been used to study the generalized stacking fault energy (GSFE) for the closed-packed (1 1 1) plane along <1 1 2>direction in FCC high entropy solid solutions$Al_xCoCrCuFeNi$ with x=0, 0.5, 1, 1.5 and 2, respectively. The GSFE curves have been calculated by the first principle. Our calculated results of the GSFEs for FCC Al are agreement with previous calculation. The GSFE curves of high entropy solid solutions $Al_xCoCrCuFeNi$ are similar to which of FCC Al. The intrinsic stacking fault energy (ISFE) γ_{isf} of $Al_xCoCrCuFeNi$ with x=1 is the maximum, and with x=2 is the least. The unstable stacking fault energy (USFE) $\gamma_{us}$of $Al_xCoCrCuFeNi$ with x=1 is maximum, and with x=0 is the least. The high entropy solid solution $Al_xCoCrCuFeNi$ with x=1 has the lowest γ_{us}/γ_{isf}ratio value, so full dislocation will be observed easily.We calculated the Peierls stress by Peierls-Nabarro model with GSFE curve, the changing of Peierls stress is similar to USFE with the different mole fraction of Al.

Key words: High entropy solid solution, Generalized stacking fault energy, Intrinsic stacking fault, Unstable stacking fault energyFirst principle.

INTRODUCTION

High entropy alloys (HEAs) are a multicomponent system of 5 to 13 metallic elements with equiatomic or nearlyequiatomic compositions [1-9].The HEA AlCoCrCuFeNi was first synthesized by Yeh et al [7-11]. The most studies were about it. There are wear resistance and high-temperature compression strength of $Al_{0.5}CoCrCuFeNi$ [5]; adhesive wear behaviour of $Al_xCoCrCuFeNi$[9];microstructure characterization of $Al_xCoCrCFeNi$[12]; mechanical performance of the $Al_xCoCrCuFeNi$ [13] and so on. Theseresearches indicate that it isimpact on microstructure characterization, adhesive wear behaviour, wear resistance, tensile property, compression strength and mechanical performance by the mole fraction of Al changed. Mechanical properties of metals depend on phenomena is a hierarchical structure from atomic up to a macroscopic length scale [14]. The generalized-stacking-fault energy (GSFE), which was introduced by Vitek [14, 15], plays an important role in proposed model for the brittle-ductile transition and dislocation properties [16, 17]. However, it is possible to form material at the microscopic and nanoscopic length scales using deposition methods such as chemical vapour deposition, physical vapour deposition and molecular-beam epitaxy. In order to minimize the quantity of defect, researchers need to know the mechanisms of dislocation nucleation, possibly leading to a criterion that determines when a dislocation will be created.

The GSFE is the interplanar potential energy for sliding one half of a crystal over the other half. Returning to the issue of dislocation nucleation in a crystal, it is desirable to know the shape of the entire GSFE curve, and to use it in a criterion for nucleation. Currently, such a potential can nowadays be determined from the embedded atom method (EAM), molecular dynamics (MD) calculations, and first-principles calculations [18].The first-principles method has been successful in calculating the grains [19], so more accurate investigation of GSFE for FCC metals is needed.For example, Wu et. al calculated the generalized stacking fault surfaces and surface energies for FCC metals by first principle [18]; Muzyk et. al calculated the generalized stacking fault energy in aluminium alloys by first principle [20]; Wang et. al calculated the dislocation properties in magnesium by first principle [21]; Yan et. al calculated the generalized stacking fault energy and dislocation properties in BCC Fe by first principle [22], and so on.

The energy-displacement curve, known formally as the GSFEcurve and introduced by Vitek [15, 23], cannot be measured experimentally except for a single point known as the intrinsic stacking fault energy (ISFE) γ_{sf} . The simulation region was

To whom all correspondence should be sent:

E-mail: yaoshan@dlut.edu.cn

rectangular with faces in the <1 1 2>, <1 1 0> and <1 1 1> directions. Periodic boundary conditions were used in the <1 1 2> and <1 1 0> directions; the (1 1 1) faces was free. The lattice was divided in half (cut by a (1 1 1) plane), with the lower-half remaining fixed and the upper-half displaced in the <1 1 2> direction in small increments. The average energy/atom was used to calculate energy per unit area of the slip plane. For slip in some directions, such as the <1 1 2> directions of a FCC crystal, positions exist at which the lattice is stable, although the crystal is not in its bulk equilibrium structure. This stable configuration is known as the intrinsic stacking fault (ISF). So slip in the <1 1 2> directions is common because the unstable stacking fault energy (USFE) γ_{us} is the lowest in those directions [24].

In this paper, we present the GSFE for (1 1 1) plane <1 1 2>directionin FCCstructure using first-principle calculations employing CASTEP package for high entropy solid solution $Al_xCoCrCuFeNi$ with x= 0, 0.5, 1, 1.5 and 2, respectively. The slab calculation is used to obtain the GSFE curves for FCC structures. Then the Peierls stresses were calculated by Peierls-Nabarro model with GSFE curves.

COMPUTATIONAL METHOD

The total-energy calculations based on the density functional theory (DFT) embodied in the CASTEP package [25] are employed in the present study. The Perdew-Burke-Ernzerhof (PBE) [26] exchange-correlation functional for the generalized-gradient-approximation (GGA) [27]is used. A plane-wave basis set is employed within the framework of the projector augmented wave (PAW) method [28, 29]. The ion-electron interaction was modeled using norm-conserving pseudopotentials [30]. The model of high entropy solid solution AlxCoCrCuFeNi with x=0, 0.5, 1, 1.5, and 2 was built using the virtual crystal approximation (VCA) [31-33]. On the basis of tests, it is chosen the energy cut-off 250eV. For first-Brillouin-zone integrals, reciprocal space is represented by Monkhorst-Pace-special k point scheme[34] with 2×4×3 grid meshes for FCC structure. The equilibrium theoretical lattice structure is determined by minimizing the Hellmann-Feynman force on the atoms and stress on the unit cell. The convergence of energy is 2×10-5eV. In the present study, we calculated the GSFE curve for the <1 1 2> direction, since the slip between the closed-packed surface is most easily for FCC Al. The ideal FCC structure closed-packed surfaces have the configuration ……ABCABC…… stacking sequence of the atomic planes. To simulate the block shear process we use a slab consisting of 6 atomic layers in the <1 1 2> direction. Between periodically repeated slab the vacuum gap 15Å normal to (1 1 1) plane is chosen to avoid interactions between two slabs.

RESULTS AND DISCUSSION

First, we calculated the GSFE curve of FCC Al, shows the GSFE curve along 1/6 <1 1 2> direction in FCC Al. The energy minimum value corresponds to the ISFE, where a full dislocation dissociates into a pair of Shockley partials. The energy maximum value is the USFE, which represents the lowest energy barrier for dislocation nucleation [18]. The trend of GSFE curve for the <1 1 2> direction in FCC Al crystal was agreement with previous calculation [17, 24, 35-40]. As can be seen from Fig. 1, it is found that γus and γisf are 144 and 100mJ/m2 for FCC Al, respectively. Table 1 lists the corresponding unstable and intrinsic stable stacking fault energies for FCC Al along with other calculated values published in literature[39, 41-43].

These indicated that the set was reasonable. So we calculated the GSFE for the <1 1 2> direction in FCC high entropy solid solution AlxCoCrCuFeNi with x=0, 0.5, 1, 1.5 and 2, respectively.

Using above set, we calculated the GSFE curve of the high entropy solid solution $Al_xCoCrCuFeNi$ with x= 0, 0.5, 1, 1.5 and 2, respectively. Fig. 1 showed the GSFE curve along 1/6 <1 1 2> direction in FCC high entropy solid solution $Al_xCoCrCuFeNi$ with x=0, 0.5, 1, 1.5 and 2, respectively. It is foundfrom Fig. 1 that theGSFE of the high entropy solid solution $Al_xCoCrCuFeNi$ with x=1 is the largest at the same slide place, it indicate that the high entropy solid solution $Al_xCoCrCuFeNi$ with x=1 is difficult to slide, so its plastic property is better than the others high entropy solid solutions.

To further study the ISFE and USFE, Fig. 2(a) shows the ISFE and USFE of the high entropy solid solution $Al_xCoCrCuFeNi$, respectively. The calculated USFEs and ISFEs are listed in Table 1. With the values of γ_{us} and γ is increasing, the potential barrier to form the stacking fault increased, and therefore it is difficult to form the stacking fault, and it is not easily deformed. It is normally that the stacking fault energy is closely related to the plastic deformation of the materials. The material having low stacking fault energy which can easily produce large plastic deformation slip dislocations further excited by twinning, and it is difficult to form stacking fault due to the high stacking fault energy, so the material having high stacking energy is poor

plastic deformability. However, it is found from Fig. 2 (a) that when the mole fraction of Al is 1, the ISFE and the USFE are the maximum. The ISFE is conducive to further stimulate the dislocation slip to improve the mechanical properties of materials. The ISFE and USFE increase first and then decrease by mole fraction of Al increasing, it indicate that the potential barrier which to form stacking fault is increased when the ISFE and USFE are increased, so it is difficult to form stacking fault, and is not easily deformed. For all high entropy solid solutions, the AlCoCrCuFeNi has the best plastic property due to the largest ISFE and USFE. It has been known that the deformation mechanism in crystals cannot be explained by the absolute value of ISFE γisf alone [44].

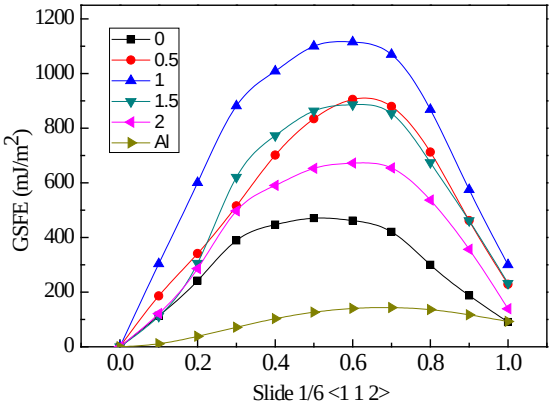

Fig.1. The GSFE curve along 1/6 the <1 1 2> direction for FCC Al and FCC high entropy alloy $Al_xCoCrCuFeNi$ with x=0, 0.5, 1, 1.5 and 2, respectively.

Although γ_{us} is not commonly used as fitting parameter for empirical potentials, the GSFE curves show the same qualitative trends for each type of materials. However, when applying a constant stress resulting in similar strain rates for both potentials, similar deformation mechanisms are observed, underlining the importance of the ratio of $\gamma us/\gamma$ is and not the absolute value of γisf [18, 44]. Although the stacking fault energy is higher, full dislocation will be observed more easily, but when this ratio is large, the energy increase necessary for nucleating the trailing partials substantial.

The value of ratio is more low, the more easy to generate dislocations, otherwise easy to generate partial dislocations.

Fig. 2(b) shows the ratios of γ_{us}/γ is for the high entropy solid solution $Al_xCoCrCuFeNi$. It is found that the ratio was the least when the mole

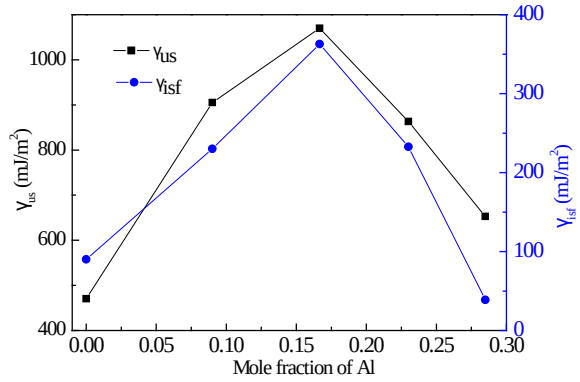

(a) The USFE and ISFE for the high entropy solid solutions $Al_xCoCrCuFeNi$

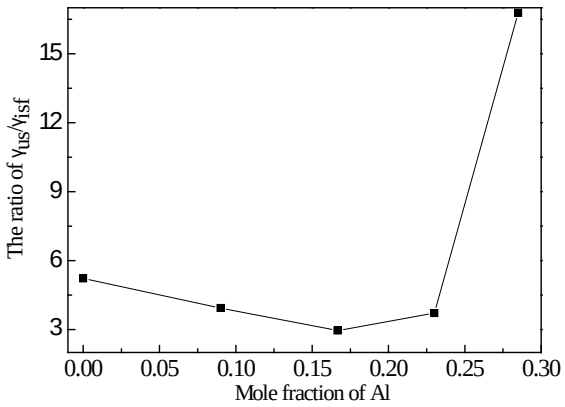

(b) The ratio of γ_{us}/γ_{isf} for the high entropy solid solutions $Al_xCoCrCuFeNi$

Fig.2. The USFE, ISFE andratio of γus/γisf of the high entropy solid solution AlxCoCrCuFeNi

fraction of Al is 1, it indicate that the high entropy solid solution AlCoCrCuFeNi may generate dislocation easily, then when the mole fraction of Al is 0 or 2, although the ISFE γ is little, it is hard to generate dislocation, because the ratio of γus/γ is is large, especially mole fraction of Al is 2 for FCC high entropy alloy $Al_xCoCrCuFeNi$.

To describe the dislocation profile and other properties related to the core of a dislocation the atomic scale discreteness has to be considered. Peierls-Nabarro (P-N) [45-47] model provides a conceptual framework and combined with atomic forces derived from the GSFE. The PN model for planar dislocations provides a continuum solution for the dis-registry of the dislocation from which a misfit energy can be computed and thus also energy barriers and stresses for dislocation motion. In the PN model, a dislocation is introduced into a lattice and it generates stresses at the interface/glide plane which are calculated according to elasticity theory.

The elastic stresses are restored by atomic forces acting on either side of the glide plane due to the misfit of atomic planes[48]. First, we calculated the lattice parameters and elastic constants of FCC Aland high entropy solid solutions $Al_xCoCrCuFeNi$by first-principle, the results were listed in Table 2. The anisotropic factor depends on the elastic constants. It is noticed that the anisotropic factor of FCC Al or high entropy solid solutions are not 1, so we calculated the Peierls stress of FCC Al and high entropy solid solutions $Al_xCoCrCuFeNi$ with improved P-N model [21, 49]. The calculated results and yield strengths are listed in Table 3. We found from Table 3 that the Peierls stresses of all the high entropy solid solutions are larger than FCC Al, it indicate that the yield strengthsof high entropy solid solution is larger than FCC Al, so the high entropy solid solution is difficult to yield, which is better than FCC Al. The Peierls stresses and yield strengths of high entropy solid solutions $Al_xCoCrCuFeNi$ with the different mole fraction of Al are shown in Fig. 3.

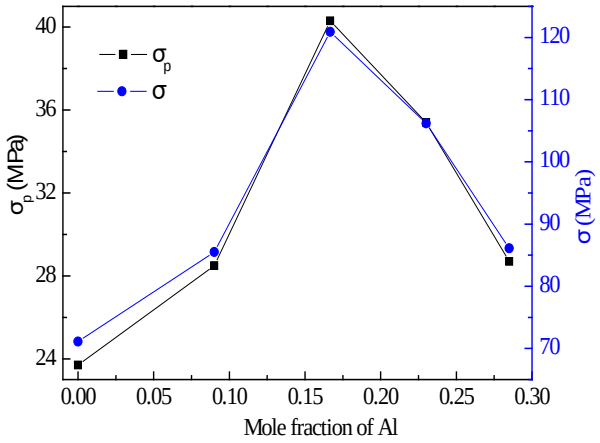

Fig. 3. The Peierls stress and yield strength of high entropy solid solutions $Al_xCoCrCuFeNi$.

It is noticed that the changing of Peierls stress with the different mole fraction of Al is similar to the USFE, this can explain that Peierls stress increases with the USFE increased [38, 50, 51,52].

Table 1. Unstable and intrinsic stacking fault energies calculated in the present work for FCC Al and previously published literature values, and the calculated values for high entropy solid solutions AlxCoCrCuFeNi. All values are given in mJ/m^2.

	γ_{us} (mJ/m^2)	γ_{isf}(mJ/m^2)	Reference
	144	100	This work
	178 [a]	146 [a]	Brandl et al. [39]
Al	129 [b]	126 [b]	Jahnaek et al. [41]
	162 [c]	130 [c]	Kibet et al. [42]
	140 [d]	112 [d]	Jin and Dunham [43]
$Al_0CoCrCuFeNi$	470.4	90.1	This work
$Al_{0.5}CoCrCuFeNi$	905.4	230.1	This work
$Al_1CoCrCuFeNi$	1070.1	362.8	This work
$Al_{1.5}CoCrCuFeNi$	863.3	232.6	This work
$Al_2CoCrCuFeNi$	652.8	38.9	This work

a. Ref. [39]: using VASP-PAW-GGA; b. Ref. [41]: using VASP-US-GGA;

c. Ref. [42]: using VASP-PAW-GGA; d. Ref. [43]: using VASP-PAW-GGA, NEB-DFT method.

Table 2. The lattice parameters, elastic constants and anisotropy factor of FCC Al and high entropy solid solutions $Al_xCoCrCuFeNi$

	a (Å)	C_{11} (GPa)	C_{12} (GPa)	C_{44} (GPa)	$A=2C_{44}/(C_{11}-C_{12})$
Al	4.05	114.3	61.92	31.62	1.21
$Al_0CoCrCuFeNi$	3.57	359.1	156.6	182.5	1.81
$Al_{0.5}CoCrCuFeNi$	3.49	699.8	228.9	321.4	1.36
$Al_1CoCrCuFeNi$	3.48	888.1	292.7	288.7	0.97
$Al_{1.5}CoCrCuFeNi$	3.51	941.6	303.3	174.9	0.54
$Al_2CoCrCuFeNi$	3.59	323.8	442.2	-339.1	5.72

Table 3. The Peierls stress of FCC Al and high entropy solid solutions $Al_xCoCrCuFeNi$.

	σ_p (MPa)	σ_s (MPa)
Al	12.2	36.6
$Al_0CoCrCuFeNi$	23.7	71.1
$Al_{0.5}CoCrCuFeNi$	28.5	85.5
$Al_1CoCrCuFeNi$	40.3	120.9
$Al_{1.5}CoCrCuFeNi$	35.4	106.2
$Al_2CoCrCuFeNi$	28.7	86.1

CONCLUSION

In conclusions, we present ab initio calculations on the GSFE on <1 1 2> directions for the closed-packed (1 1 1) plane in FCC high entropy solid solutions $Al_xCoCrCuFeNi$. The density functional theory (DFT) within generalized gradient approximation (GGA) is employed. Our values of the GSFEs are in better agreement with previous calculated results. The calculated results indicate that the USFE γus and ISFE γisf of FCC high entropy alloy $Al_xCoCrCuFeNi$ with x = 1 is the maximum. We analyze the ratio of γus/γisf and positions for the ISF and USF. The high entropy solid solution $Al_xCoCrCuFeNi$ with x=1 has the lowest γus/γisfratio value, so full dislocation will be observed easily.The calculated results of Peierls stresses indicate the high entropy solid solutions are difficult to yield, which is better than FCC Al.

REFERENCES

1. T. Masuko, A. Minami, N. Iwasaki, T. Majima, S. Nishimura, Y. C. Lee, *Anal Biochem.*, **69**, 339 (2005).
2. S. Ranganathan, *Current Science*., **85,** 1404 (2003).
3. L. Liu, J. Zhu, C. Zhang, J. Li, Q. Jiang, *Materials Science and Engineering*., **64**, 548 (2012).
4. X. Yang, Y. Zhang, P. Liaw, *Procedia Engineering*, **36**, 292 (2012).
5. Y. Zhang, X. Yang, P. Liaw, *JOM*, **64,** 830 (2012).
6. C.Y. Hsu, J. W. Yeh, S.K. Chen, T.T. Shun, *Metallurgical and Materials Transactions A*, **35,** 1465 (2004).
7. J.W. Yeh, S.K. Chen, S.J. Lin, J.Y. Gan, T.S. Chin, T.T. Shun, C.H. Tsau, S.Y. Chang, *Advanced Engineering Materials.*, **6**, 299 (2004).
8. J.W. Yeh, S.J. Lin, T.S. Chin, J.Y. Gan, S.K. Chen, T.T. Shun, C.H. Tsau, S.Y. Chou.*Metallurgical and Materials Transactions A*, **35,** 2533 (2004).
9. P.K. Huang, J.W. Yeh, T.T. Shun, S.K. Chen, *Advanced Engineering Materials*, **6,** 74 (2004).
10. J.M. Wu, S.J. Lin, J.W. Yeh, S.K. Chen, Y.S. Huang, H.C. Chen, *Wear.*, **261,** 513 (2006).
11. C.C. Tung, J.W. Yeh, T.t. Shun, S.K. Chen, Y.S. Huang, H.C. Chen, *Materials letters.*, **61,** 1 (2007).
12. S. Singh, N. Wanderka, B. Murty, U. Glatzel, J. Banhart, *ActaMaterialia*, **59,** 182 (2011).
13. C.J. Tong, Y.L. Chen, J.W. Yeh, S.J. Lin, S.K. Chen, T.T. Shun, C.H. Tsau, S.Y. Chang, *Metallurgical and Materials Transactions A*, **36,** 881 (2005).
14. C.J. Tong, M.R. Chen, J.W. Yeh, S.J. Lin, S.K. Chen, T.T. Shun, S.Y. Chang, *Metallurgical and Materials Transactions A*, **36,** 1263 (2005).
15. V. Vitek, *Lattice Defects*, **5**, 1 (1974).
16. V. Vitek, *Philosophical Magazine*, **18,** 773 (1968).
17. R. Thomson, *Physical Review B*, **52,** 7214 (1995).
18. Y. Sun, E. Kaxiras, *Philosophical Magazine A*, **75,** 1117 (1997).
19. X.Z. Wu, R. Wang, S.F. Wang, Q.Y. Wei, *Applied Surface Science*, **256,** 6345 (2010).
20. R.W. X.Z. Wu, S.F. Wang, *Applied Surface Science*, **256**, 3409 (2009).
21. M. Muzyk, Z. Pakiela, K. Kurzydlowski, *ScriptaMaterialia*, **64,** 916, (2011).
22. R. Wang, S.F. Wang, X.Z. Wu, Q.Y. Wei, *PhysicaScripta*, **81,** 601 (2010).
23. J.-A. Yan, C.-Y. Wang, S.Y. Wang, *Physical Review B*, **70,** 105 (2004).
24. V. Vitek. *Physica Status Solidi.*, **18,** 687 (1966).
25. J.A. Zimmerman, H. Gao, F.F. Abraham, *Modelling and Simulation in Materials Science and Engineering*, **8,** 103 (2000).
26. M. Segall, P.J. Lindan, M. Probert, C. Pickard, P. Hasnip, S. Clark, M. Payne, *Journal of Physics*, **14,** 2717 (2002).
27. J.P. Perdew, K. Burke, M. Ernzerhof.*Physical review letters*, **77,** 3865 (1996).
28. M.C. Payne, M.P. Teter, D.C. Allan, T. Arias, J. Joannopoulos, *Reviews of Modern Physics*, **64,** 1045 (1992).
29. P.E. Blöchl, *Physical Review B*, **50**, 17953 (1994).
30. G. Kresse, D. Joubert, *Physical Review B*., **59**, 1758, (1999).
31. 30. D. Hamann, M. Schlüter, C. Chiang. *Physical Review Letters*, **43**, 1494 (1979).
32. L. Bellaiche, D. Vanderbilt, *Physical Review B*, **61**, 7877 (2000).
33. B. Winkler, C. Pickard, V. Milman, *Chemical Physics Letters*, **362**, 266 (2002).
34. J.M. Larkin, A.J. McGaughey, *J. Appl. Physics*, **114**, 023507 (2013).
35. H.J. Monkhorst, J.D. Pack, *Physical Review B*, **13**, 5188 (1976).
36. G. Lu, N. Kioussis, V.V. Bulatov, E. Kaxiras, *Physical Review B*, **62**, 3099 (2000).
37. S. Ogata, J. Li, S. Yip, *Science*, **298,** 807 (2002).
38. P. Denteneer, J. Soler, *Solid State Commun.*, **78**, 857 (1991).
39. J. Hartford, B. Von Sydow, G. Wahnström, B. Lundqvist, *Physical Review B*, **58**, 2487 (1998).
40. C. Brandl, P. Derlet, H. Van Swygenhoven, *Physical Review B*, **76**, 54 (2007).
41. A.F. Wright, M.S. Daw, C. Fong, *Phil. Magazine A*, **66**, 387 (1992).

42. M. Jahnátek, J. Hafner, M. Krajčí, *Physical Review B*, **79**, 224103 (2009).
43. S. Kibey, J. Liu, D. Johnson, H. Sehitoglu, *ActaMaterialia*, **55**, 6843 (2007).
44. Z. Jin, S. Dunham, H. Gleiter, H. Hahn, P. Gumbsch, *ScriptaMaterialia*., **64**,605 (2011).
45. H. Van Swygenhoven, P. Derlet, A. Frøseth, *Nature Materials*, **3**, 399 (2004).
46. R. Peierls.*Proc. Phys. Soc.*, **52**, 34 (1940).
47. F. Nabarro, *Proceedings of the Physical Society*, **59**, 256 (1947).
48. J.P. Hirth, J. Lothe, *Theory of Dislocations*, **12,** 127 (1982).
49. B.v. Sydow, J. Hartford, G. Wahnström, *Computational Materials Science*, **15**, 367, (1999).
50. S.F. Wang, *Journal of Physics A: Mathematical and Theoretical*, **42**, 025208 (2009).
51. O.N. Mryasov, Y.N. Gornostyrev, *Physical Review B*, **58**, 11927 (1998).
52. W. Xiao-Zhi, W. Shao-Feng, L. Rui-Ping, *Chinese Physics B*, **18**, 2905 (2009).